COBEM 2023 27TH INTERNATIONAL CONGRESS OF MECHANICAL ENGENEERING

ABCM Brazilian Society of Mechanical Sciences and Engineering
27th ABCM International Congress of Mechanical Engineering
December 04-08, 2023, Florianópolis-SC, Brazil

COBEM-2023-0809
EVALUATION OF TENSILE STRENGTH ANISOTROPY IN PREFORMS OF AUSTENITIC STAINLESS STEEL 316L-SI OBTAINED BY WIRE ARC ADDITIVE MANUFACTURING

Igo Jose Silva Azevedo
Júlio Feitosa da Silva Neto
Joyce Ingrid Venceslau de Souto
Yuri Emanoel Pereira Dias
Gabriel de Castro Coêlho
Federal University of Campina Grande – Campina Grande PB
igo.jose@estudante.ufcg.edu.br, julio.feitosaneto@estudante.ufcg.edu.br, joyce.ingrid@estudante.ufcg.edu.br, yuri.dias@copin.ufcg.br, gabriel.coelho@estudante.ufcg.edu.br

Jefferson Segundo de Lima
Federal University of Pernambuco – Recife PE
jefferson.segundo@ufpe.br

Abstract. *The Additive Manufacturing (AM) process can generate intricate geometries, making it ideal for crafting components with complex internal and external structures, as well as for swiftly producing objects within a short timeframe. In this scenario, items are formed through the layer-wise addition of materials, which can consist of polymer filaments or steel. Among the primary alloys employed in Wire Arc Additive Manufacturing (WAAM), austenitic stainless-steel alloys stand out, finding extensive applications in the transportation, gas, and oil industries due to their mechanical strength and corrosion resistance properties. In this context, the objective of this study is to assess the anisotropy of tensile strength in preforms of austenitic stainless steel 316L-Si obtained through WAAM. The anisotropic evaluation was conducted based on tensile tests, wherein the bond strength of the depositions was appraised. To execute the tensile test, three samples of the specimen were taken in the vertical and horizontal directions, as well as at a 45° angle concerning the direction of the deposited layers. The principal outcomes gleaned from the anisotropic assessment suggest that the specimen removed parallel to the direction of metal deposition (longitudinal direction) exhibits higher tensile strength, whereas specimens removed transversely to the direction of layer deposition reveal critical points and, consequently, lower tensile strength.*

Keywords: *Additive Manufacturing, WAAM, Austenitic stainless steel 316L-Si, Tensile strength, Mechanical properties, Anisotropy.*

1. INTRODUCTION

Additive Manufacturing (AM) is defined as a group of technologies that utilize a layer-by-layer approach to create objects with a free form, also known as 3D printing (Sommer; Blumenthal, 2019). AM is an evolution of rapid prototyping in that it creates a physical product from a 3D CAD digital file. This technique involves designing a component in layers, and these multiple layers are deposited through welding processes, producing the component without the need for molds or other tools. AM has shown a path for the scientific and industrial community toward the direct formation of products and has also replaced traditional approaches in some industrial contexts by minimizing material consumption. AM constructs one by the deposition of materials, these depositions are layer by layer, in which the layers begin on a substrate as practiced in conventional subtractive manufacturing. AM is a promising alternative for the manufacturing of components made from expensive materials, such as titanium and nickel in the aerospace industry, where such components typically undergo an extremely high buy-to-fly ratio.

Since the AM process manufactures a part with complex geometry through the deposition of weld beads layer by layer, it is important to model the geometry of a single weld bead, as well as the overlap process of multiple beads, in order to achieve high surface quality and dimensional accuracy of the manufactured parts (Ding et al., 2015). Initially, this technology was almost restricted to high-energy density processes; however, the pursuit of greater competitiveness has led to the use of arc welding processes, using additive material in wire form. This technology enables the creation of complex and customized parts, layer by layer, based on a digital model. The challenges involved in the manufacturing of components by AM, both in the deposition of multiple layers and in the finishing phase, are highlighted.

Among stainless steel alloys, the AISI 316L alloy is one of the most sought after in the oil and gas industry due to its excellent characteristics for the sector. Austenitic stainless steels, such as 316L, are a group of materials commonly used

in AM processing, which are suitable, for example, for applications involving high-performance parts due to their good mechanical properties. Among the austenitic stainless steels, 316L-Si steel has emerged as a promising option for engineering applications.

The AM process enters the oil and gas sector with the purpose of addressing several limitations left by conventional manufacturing processes. In AM, each layer is manufactured through the deposition of a large number of single weld beads side by side. Therefore, it is important to investigate the process of overlapping deposits with multiple beads (Ding et al., 2015). However, a significant challenge in metal AM is the anisotropy of tensile strength, that is, the variation in mechanical properties. The quality and integrity of the produced parts still pose a challenge for researchers and professionals in the field. Evaluating the anisotropy of tensile strength in metal preforms produced by AM is a topic of great significance to ensure the safety and reliability of these components.

Anisotropy can occur due to the microscopic structure and crystalline orientation resulting from the AM process, which can lead to variations in mechanical properties along different directions of the part. Tensile strength anisotropy is a significant concern as it can affect the structural integrity and mechanical performance of additively manufactured parts in critical applications. In this context, the assessment of tensile strength anisotropy in austenitic stainless steel 316L-Si preforms obtained by AM has become a relevant research topic.

This work aims to conduct a study on AM with an emphasis on the use of arc processes. The primary focus will be on evaluating the mechanical performance of walls constructed via AM, utilizing weld depositions layer by layer. Additionally, the study will address the anisotropy of tensile strength in austenitic stainless steel 316L-Si preforms obtained through AM.

2. METHODOLOGY

The preform layers were manufactured in the Welding Laboratory (LabSol) of the UAEM at UFCG. The process was produced through a three-axis robotic system controlled by the MACH3 software for CNC. The construction process involved MIG welding, which utilizes an electric arc to melt the wire onto the base material. The AM was performed using the Gas Metal Arc Welding (GMAW) process, which employs an electric arc established between an electrode and the workpiece, promoting the fusion of the wire by the electric arc.

The material used for the welding wire was austenitic stainless steel 316L, as shown in Table 1. The robot was responsible for the precise movement of the welding torch and the execution of programmed commands.

Table 1. Composition of 316L Steel.

		C	Mn	Si	P	S	Cr	Mo	Ni	N
wire	MIN	-	-	-	-	-	16	2	10	-
	MAX	0,03	2	0,75	0,045	0,03	18	3	14	0,10

In Figure 1 illustrates the schematics of the robot for AM. The welding power source used was the Digiplus A7 from IMC, configured in Short-Circuit transfer mode. The shielding gas employed was argon, ensuring proper protection of the arc and the weld pool.

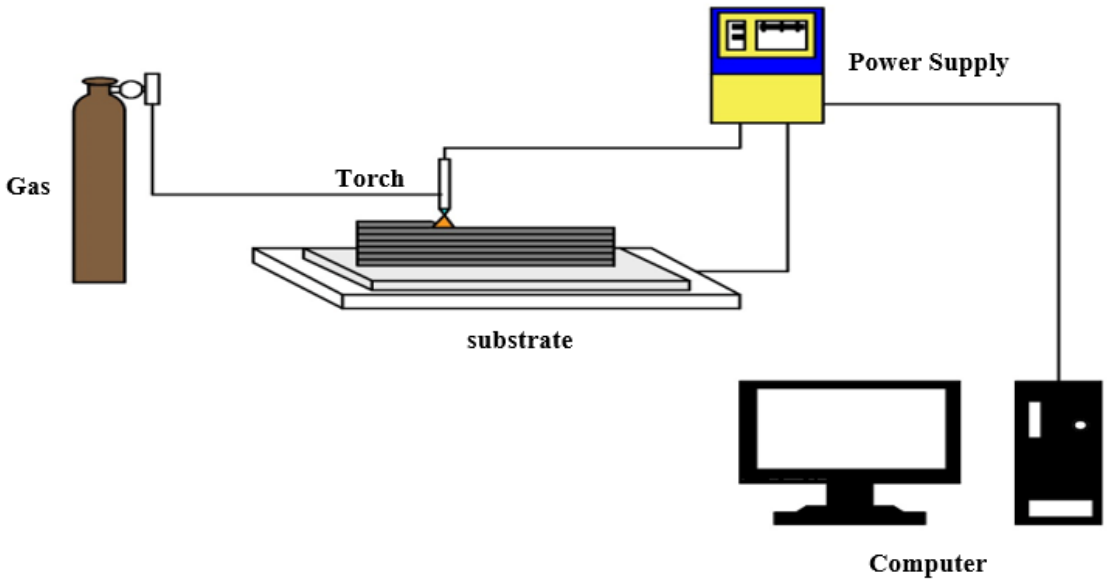

Figure 1. Schematic of the WAAM equipament.

The substrate was adequately cleaned and prepared, ensuring a surface free of impurities and oxidation before welding. Based on specialized literature and preliminary tests, the ideal welding parameters were selected, including current, voltage, wire feed speed, and shielding gas flow rate (see Table 2). Using the MACH3 software for CNC, the robot movements were programmed to ensure the precise deposition of the layers, where molten metal droplets were transferred to the weld pool through the electric arc.

The layers, as depicted in Figure 2, deposited using the controlled short-circuit transfer mode, are characterized by a welding process in which molten metal droplets are transferred to the weld pool through controlled electrical short-circuits. In this transfer mode, the electric arc is periodically interrupted, resulting in a short-circuit between the electrode and the weld pool. This short-circuit creates a rapid and controlled transfer of molten metal droplets, contributing to a smooth and uniform deposition of the layers.

Figure 2. Complete appearance of a component obtained by WAAM.

The wall obtained by WAAM was initially machined to achieve a thickness of 2 mm, as shown in Figure 3. The machining process was carried out precisely, ensuring that the plate exhibited the desired thickness uniformly across its entire extent. This machining step is crucial to ensure dimensional consistency and compliance with the required specifications.

Table 2. Parameters used in the process.

PARAMETERS	VALUE
Refrigeration gas	Argon
Gas flow used	18 L/min
Wire feed speed	4 m/min
Peak current	250 A
Current	180 A
Deposition speed (feed)	300 mm/min
Wire diameter	1,2 mm
Two-part distance	3 mm
Torch angle to workpiece/substrate	90°

The wall obtained by WAAM was initially machined to achieve a thickness of 2 mm, as shown in Figure 3. The machining process was carried out precisely, ensuring that the plate exhibited the desired thickness uniformly across its entire extent. This machining step is crucial to ensure dimensional consistency and compliance with the required specifications.

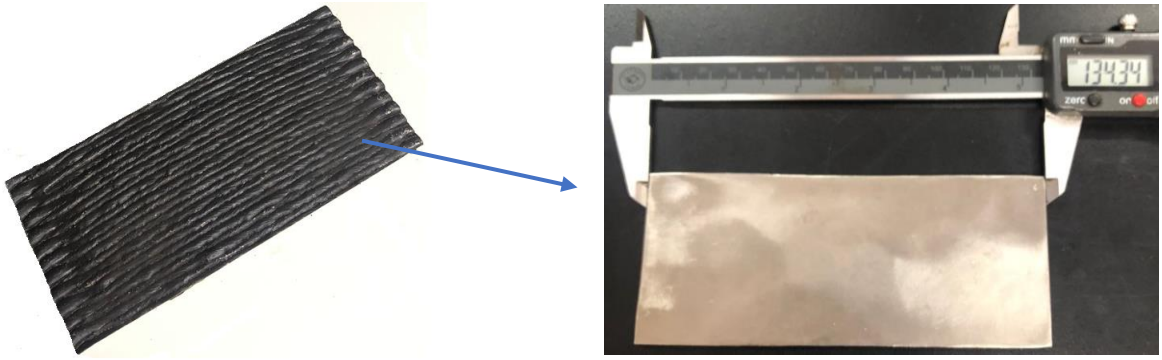

Figure 3. Appearance of a component obtained by WAAM after machining.

After the machining process, nine specimens were taken for the tensile test, three in the horizontal direction, three in the vertical direction, and three at an angle of 45° relative to the layer direction, as shown in Figure 4. Due to the AM process, mechanical properties can vary in different directions, especially when dealing with layered oriented structures.

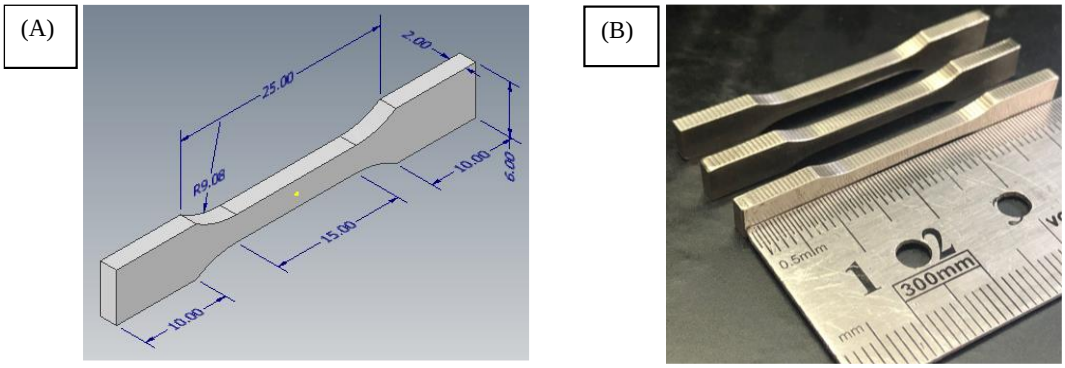

Figure 4. (A) Representation of the specimen, (B) Machined specimen.

3. RESULTS AND DISCUSSION

3.1 Microstructure

Throughout the cross-section, microscopic images depict the structure of a component manufactured by WAAM. The figure highlights the presence of ferrite (represented in shades of black) distributed within the austenite matrix (shown in gray). The Figure 5 (b) represents the upper part of the manufactured wall, Figure 5 (c) displays the central part of the layers, and Figure 5 (d) exhibits the lower part of the manufactured wall. Notably, the grain growth is predominantly in the vertical direction, indicating substantial alignment.

The upper layer of the wall is not affected by the heat from the metal buildup. Therefore, the microstructure of the upper layer could be used as the initial state for analyzing the influence of the (N + 1) depositing layer on the N-th layer. The upper layer of the AM is divided into three zones in the longitudinal direction. The upper zone is primarily cellular dendritic, where more ferrite phase is formed in the dendritic structure (Zhao et al., 2023). The microstructures were obtained from the same component. This allows for a direct analysis of the uniformity of structural properties in different regions of the manufactured wall. The images reveal consistency in the distribution of ferrite and in the vertical orientation of grain growth across the entire extent of the wall, reinforcing the quality of the WAAM manufacturing process.

During the AM process, when the (N + 1) layer is deposited, the upper part of the previous N layer is heated, melted, and mixed with the molten metal to form part of the (N + 1) layer. The unmelted part of the previous N layer becomes rougher due to the heat, but its orientation remains the same, resulting in an internal structure of the N layer with directional grains. This, in turn, presents significant issues of anisotropy in the structure. Enhancement of the anisotropic mechanical property was optimized with the application of current pulses instead of continuous currents, due to the lower heat generation and increased cooling rate, resulting in the formation of finer grains, as observed by Altor et al. (2013). The adoption of pulsed current increased the solidification rate at the casting area edge. With the accelerated solidification, there is less time available for the transformation of austenite into ferrite. Thus, the use of pulsed current is expected to result in a reduced amount of ferrite, which was also observed in the work of Tabrizi Reza et al. (2021).

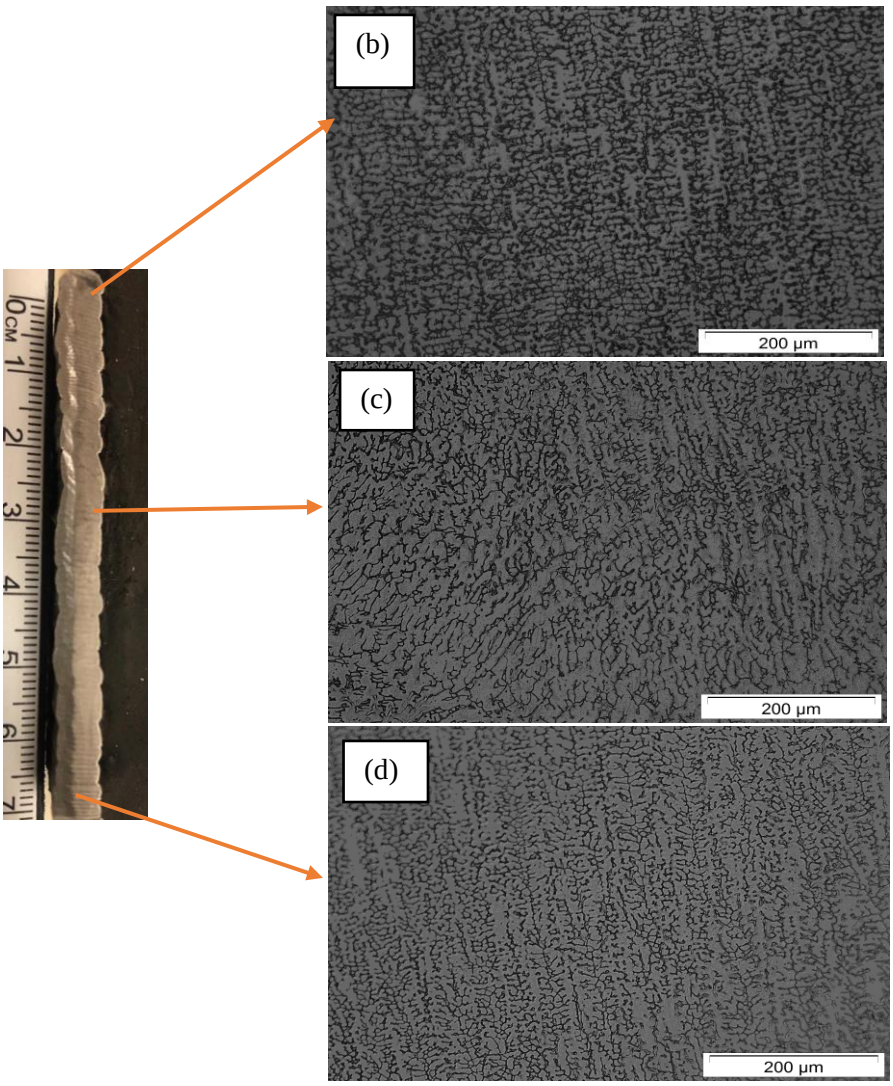

Figure 5. (a) Optical micrographs along the cross-section of a manufactured wall, produced by WAAM. (b) shows regions of the upper part. (c) shows regions of the central part, and (d) shows regions of the lower part of the wall.

3.2 Tensile Strength

Upon analyzing Figure 6, parameters such as tensile strength and toughness were observed. By comparing the results of the specimens tested in the vertical direction at 90°, horizontal at 0°, and inclined at 45° relative to the deposited layers, variations in the mechanical properties of the material were identified due to the anisotropy of the layer orientations.

The results obtained revealed that the specimen in the vertical direction at 90° exhibited higher tensile strength and lower toughness, while the inclined specimen at 45° showed the second highest tensile strength and the highest toughness. On the other hand, the horizontal specimen displayed lower tensile strength and the second highest toughness, as will be observed in Figure 6.

The specimen at 45° showed the second highest tensile strength, suggesting that the layer orientation in this direction also offers a certain advantage in terms of strength. However, the difference in strength between the vertical and 45° specimens can be attributed to factors such as load transfer efficiency and stress distribution along the specimen. Regarding toughness, it was observed that the 45° specimen achieved the highest toughness, followed by the vertical specimen. The vertical 90° specimen exhibited the lowest toughness. In this case, the 45° sample demonstrated a greater capacity to dissipate energy before reaching rupture. This characteristic can be explained by the orientation of the layers, which may allow for a better balance between strength and plastic deformation.

These variations occurred due to anisotropic effects resulting from the manufacturing process and the intrinsic properties of the material. We observed that the specimens tested in the vertical direction exhibit higher yield strength

and tensile strength compared to the specimens tested in the horizontal direction, indicating greater material strength in the vertical direction.

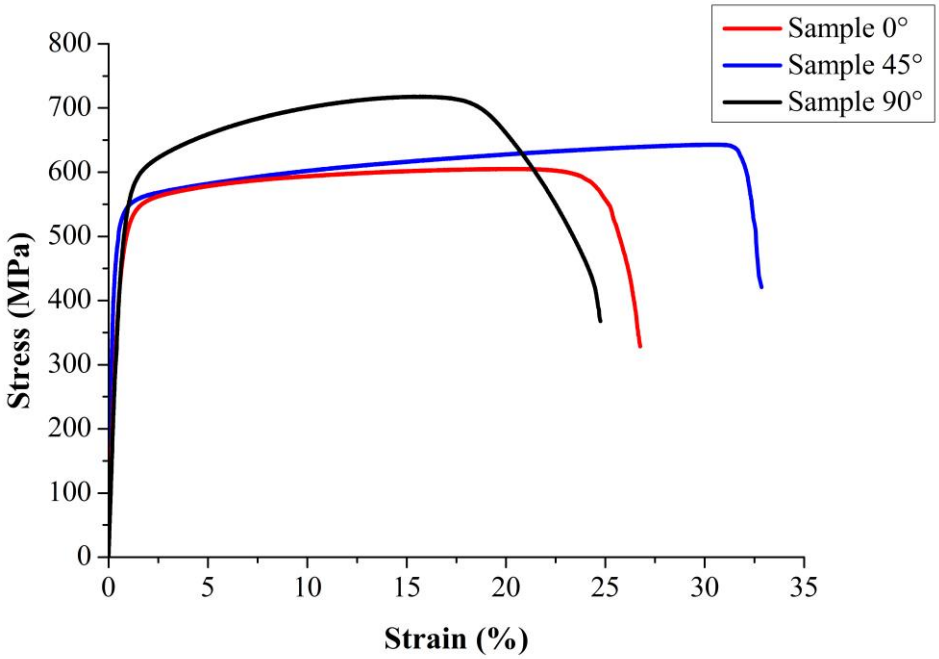

Figure 6. Stress x strain graph.

3.3 Fractography

In Figure 7, shows representative images of Scanning Electron Microscopy (SEM), including other representations of the fracture morphologies of the components produced by WAAM. Microcavities are visible with a relatively uniform distribution on the fracture surface, indicating that the fracture mode is predominantly ductile and that the formed materials exhibit excellent toughness.

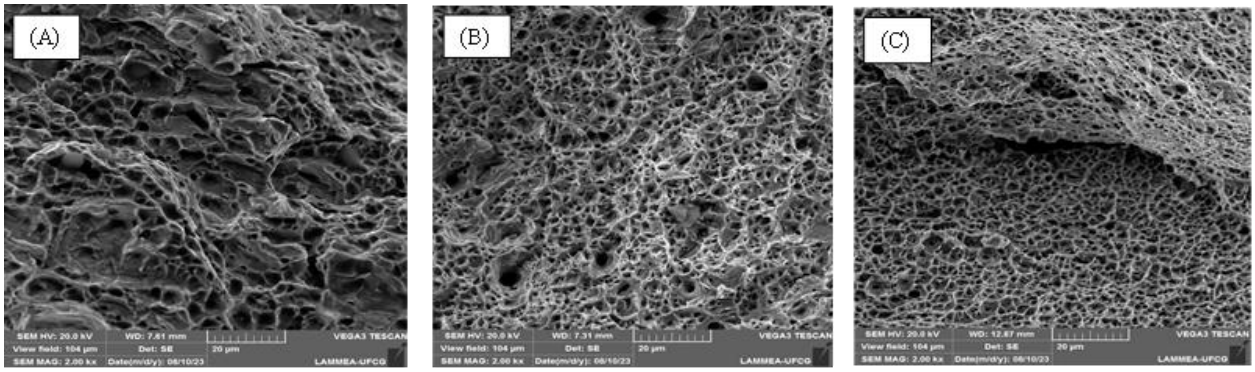

Figure 7. Scanning electron microscopy (SEM) representations of the fracture morphologies of the components produced by WAAM.

However, it could be observed that noticeable differences in the dimensions and depths of the pits between different directions of the specimens are apparent. The existence of columnar grains can lead to disparity in the direction of growth of the coarse gamma columnar grains (direction L) and in the vertical direction (direction T) (Baufeld; Biest; Gault, 2010). Based on the Hall-Petch equation, (Jia et al., 2016), there is a phenomenon of strengthening at the boundaries of two adjacent grains. The reason for the differences among the three samples is that there are fewer grain boundaries in direction L, while there are more in direction T (Wang; Xue; Wang, 2019).

4. CONCLUSIONS

Based on the results obtained from the tensile test, it can be concluded that the horizontally oriented specimen, manufactured by AM, exhibited the highest tensile strength. This greater strength can be attributed to the anisotropy of the layers resulting from the manufacturing process. Regarding toughness, the specimen inclined at 45° displayed the highest toughness, while the horizontal sample exhibited the lowest. The vertical specimen, on the other hand, demonstrated the second highest toughness. These observations indicate that the layer orientation influences not only the strength but also the material's ability to absorb energy before fracturing.

These results provide an understanding of the structural and fracture properties of components manufactured by WAAM. The uniformity in the distribution of ferrite and the vertical grain growth reinforces the quality of the manufacturing process. The differences in fracture characteristics between the directions of the specimens highlight the importance of considering orientation when evaluating the properties of materials produced by WAAM. Ultimately, strength, toughness, and other desired properties can be achieved through controlled process adjustments, enabling the production of highly effective components in a variety of applications.

It is important to emphasize that the results are specific to the austenitic 316L-Si steel manufactured by AM. Therefore, it is concluded that the orientation of the layers and the material structure influenced by the AM process play a significant role in the mechanical properties, such as tensile strength and toughness, of the austenitic 316L-Si steel.

5. ACKNOWLEDGEMENTS

The authors thank National Council for Scientific and Technological Development – CNPq for the investment and scholarship, through process: 409585/2022-0 and 408253/2022-3. To the welding, metallography, microscopy and mechanical properties characterization laboratories of the Department of Mechanical Engineering (UAEM) at the Federal University of Campina Grande (UFCG).

6. REFERENCES

Baufeld, B.; VAN D.; Biest, O.; Gault, R. “Additive manufacturing of Ti–6Al–4V components by shaped metal deposition: microstructure and mechanical properties”. *Materials & Design*, v. 31, p. S106-S111, 2010.

Barczewski, B. F. et al., Aplicações da manufatura aditiva em oftalmologia. *Revista Brasileira de Oftalmologia*, v. 81, p. e0052, 22 jul. 2022.

Ding, D., et al. "A multi-bead overlapping model for robotic wire and arc additive manufacturing (WAAM)". *Robotics and Computer-Integrated Manufacturing*, v. 31, p. 101–110, 1 fev. 2015.

Jia, Weitao et al. "Relationship between microstructure and properties during multi-pass, variable routes and different initial temperatures hot flat rolling of AZ31B magnesium alloy". *Materials & Design*, v. 103, p. 171-182, 2016.

Jun, M.; Altor, A. E.; Craft, C. B. "Effects of increased salinity and inundation on inorganic nitrogen exchange and phosphorus sorption by tidal freshwater floodplain forest soils", Georgia (USA). *Estuaries and Coasts*, v. 36, p. 508-518, 2013.

Sommer, A. C.; blumenthal, Eytan Z. "Implementations of 3D printing in ophthalmology". *Graefe's Archive for Clinical and Experimental Ophthalmology*, v. 257, p. 1815-1822, 2019.

Tabrizi, T. R. et al. "Comparing the effect of continuous and pulsed current in the GTAW process of AISI 316L stainless steel welded joint: microstructural evolution, phase equilibrium, mechanical properties and fracture mode". *Journal of Materials Research and Technology*, v. 15, p. 199-212, 2021.

Wang, L.; Xue, J.; Wang, Q. "Correlation between arc mode, microstructure, and mechanical properties during wire arc additive manufacturing of 316L stainless steel". *Materials Science and Engineering: A*, v. 751, p. 183-190, 2019.

Zhao, DongSheng et al. "Effect of Current Mode on Anisotropy of 316L Stainless Steel Wire Arc Additive Manufacturing". *Journal of Materials Engineering and Performance*, p. 1-5, 2023.

7. RESPONSIBILITY NOTICE

The authors are the only responsible for the printed material included in this paper.